A microfluidic platform for on-demand formation and merging of microdroplets using electric control

Hao Gu,[a] Chandrashekhar U. Murade, Michael H. G. Duits, and Frieder Mugele
Physics of Complex Fluids, Faculty of Science and Technology, IMPACT and MESA + Institutes, University of Twente, P.O. Box 217, 7500AE Enschede, The Netherlands

(Received 18 January 2011; accepted 27 January 2011; published online 31 March 2011)

We discuss a microfluidic system in which (programmable) local electric fields originating from embedded and protected electrodes are used to control the formation and merging of droplets in a microchannel. The creation of droplets-on-demand (DOD) is implemented using the principle of electrowetting. Combined with hydrodynamic control, the droplet size and formation frequency can be varied independently. Using two synchronized DOD injectors, merging-on-demand (MOD) is achieved via electrocoalescence. The efficiency of MOD is 98% based on hundreds of observations. These two functionalities can be activated independently. © *2011 American Institute of Physics.* [doi:10.1063/1.3570666]

In the past decade, droplet-based microfluidics have found an increasing number of applications in areas such as biomedical diagnostics, drug screening, and chemical synthesis on chip.[1–4] This technology offers several advantages such as sample volume reduction, fast reaction and analysis, low energy consumption, and increased automation. Current trends are that microfluidic chips are becoming more multifunctional and more dedicated to specific operations. The recent developments of droplets-on-demand (DOD) and merging-on-demand (MOD) functionalities connect very well to this trend. DOD is needed in applications where either the number of drops needs to be controlled or where different droplet manipulations need to be synchronized to each other. MOD can either facilitate 2D matrix screening tests or applications where the decision to merge (or not) depends on a prior diagnosis of the droplet contents. In this case, the presence of the two candidate droplets at the same time and place as required by MOD could be facilitated by DOD.

One prominent research area where DOD and MOD have strong potential is the on-chip screening of biological cells that have been encapsulated in droplets. Here, the cells may be rare and/or the reagents are costly, making it necessary to generate (and merge) droplets only when needed. Alternatively, the number of cells may also be very large, while only a few are of interest. In this case, a high throughput screening is needed in which each droplet is first analyzed for a cellular response and then given a fate (as in Ref. 5). One way to determine this fate is to merge it with another drop (or not).

Two different platforms are available for achieving DOD or MOD. In the so-called digital microfluidics (DMF), all droplet manipulations are carried out as discrete steps by switching individually addressable electrodes. Since droplet creation, transport, and merging essentially involve the same operation (activating a local electrode), the DMF platform is very well suited for both DOD and MOD. However, for applications that require high throughput or involve downstream operations that are incompatible with DMF, continuous flow microfluidics is preferred. In that case, DOD and MOD require the integration of active elements with the layout of the flow channels.

In this paper, we consider DOD and MOD in continuous flow geometries. Different ways of realizing DOD have been reported. Lin and Su[6] and Zeng *et al.*[7] described a system using pneu-

[a]Author to whom correspondence should be addressed. Electronic mail: h.gu@tnw.utwente.nl.

matic microvalves fabricated in polydimethylsiloxane (PDMS), while Churski *et al.*[8] used external valves interconnected with a microchip. Alternatively, also electric signals can be used to create droplets-on-demand. Malloggi *et al.*[9,10] used electrowetting to increase the wettability of the channel wall at the location of drop formation. With both the mechanical and the electrical methods, a certain control over droplet volume (V) and/or generation rate (k) could be achieved. However, there is still lack of an efficient on-demand platform to produce droplets using electric control.

The merging of droplets in a flow channel geometry has been widely studied for passive methods,[11–13] which do not require intervention and always result in fusion. In contrast, MOD has been studied only a few times. Link *et al.*[14] reported that droplets can be merged by applying dc voltages with opposite sign across the two droplets during their formation. Priest *et al.*[15] and Wang *et al.*[16] demonstrated MOD applications based on electrocoalescence (EC) using dc or ac voltages. However, each method required a precise droplet synchronization and precise electrode alignment. A different EC-based MOD method was reported by Zagnoni and Cooper.[17–19] They used a pattern of electrodes to hold a single droplet at the channel surface until the second one arrived. This worked successfully after a careful tuning of the flow strength. However, in these EC applications where electrodes were in direct contact with the fluid, the occurrence of electrochemical reactions seems hard to exclude. This could be disadvantageous especially in bioanalytical applications, where, depending on the biological content, redox reactions could occur.

While the results of these initial studies are certainly promising, it is also clear that the demand for new DOD/MOD systems is expected to remain for some time. First of all, the diversity of potential applications is rather large, which means that certain types of implementation (electric and mechanical) will go well with certain types of microfluidic chip. Second, also aspects, such as the ease of manufacturing or the robustness of the device, will drive the development of new designs.

In this paper, we present a DOD and MOD device that is easy to manufacture, requiring merely a patterning of electrodes, dip-coating, and soft lithography. DOD and MOD electrodes are integrated in the same layer and can be activated independently. The footprint is small, which facilitates parallelization of multiple DOD injectors and MOD mergers, thus allowing also more complex operations (e.g., multiple mixing or dilution steps). Since our chip contains no moving parts and its electrode surfaces are protected against electrolysis by an insulator layer, it has the potency to become a robust chip.

As shown in Fig. 1(a), our system is based on the combination of microchannels and insulator-covered electrodes. The channels are fabricated in PDMS using single-layer soft lithography. Electrodes are obtained by depositing indium tin oxide (ITO) on a glass substrate and etching part of the ITO away with 18% HCl via the standard wet etching method.[20] Then the patterned ITO-glass is covered with a (d=) 3.2 μm thick Teflon AF insulator layer via dip-coating.[21] The chip is assembled by clamping the PDMS structure onto the Teflon covered substrate. Flow-focusing geometry is used for the channel layout for droplet formation. The dimensions are a channel height of 50 μm and a width of 100 μm for the main channel and 50 μm for the orifice. The chip is mounted on the stage of an inverted microscope (TE 2000U, Nikon, Japan), equipped with a high speed camera (Photron FASTCAM SA3, Japan).

Our dispersed phase (W) consists of de-ionized water plus NaCl (conductivity: 5 mS/cm), while our continuous phase (O) is mineral oil plus 3 wt % (nonionic) Span 80 surfactant. The inlet pressures P_W and P_O can be tuned using hydrostatic heads and are kept at 4.8 and 7.5 kPa, respectively. Electric fields are applied by connecting ITO electrodes to ac voltage sources (10 kHz), while the aqueous phase reservoir is connected to the ground.

Droplet on-demand capabilities are first explored using continuous ac voltage. Results are shown in Figs. 1(b) and 1(c). Below a root-mean-square voltage (U_{rms}) of $\approx$30 V, no droplets are formed. Increasing U_{rms} up to 70 V, the drop generation frequency k grows from 1.5 to 10 Hz (voltages in excess of 70 V lead to contact line instabilities and polydisperse droplets). Remarkably, the droplet diameter (D) remains fairly constant at $\approx$50 μm. This trend differs from the

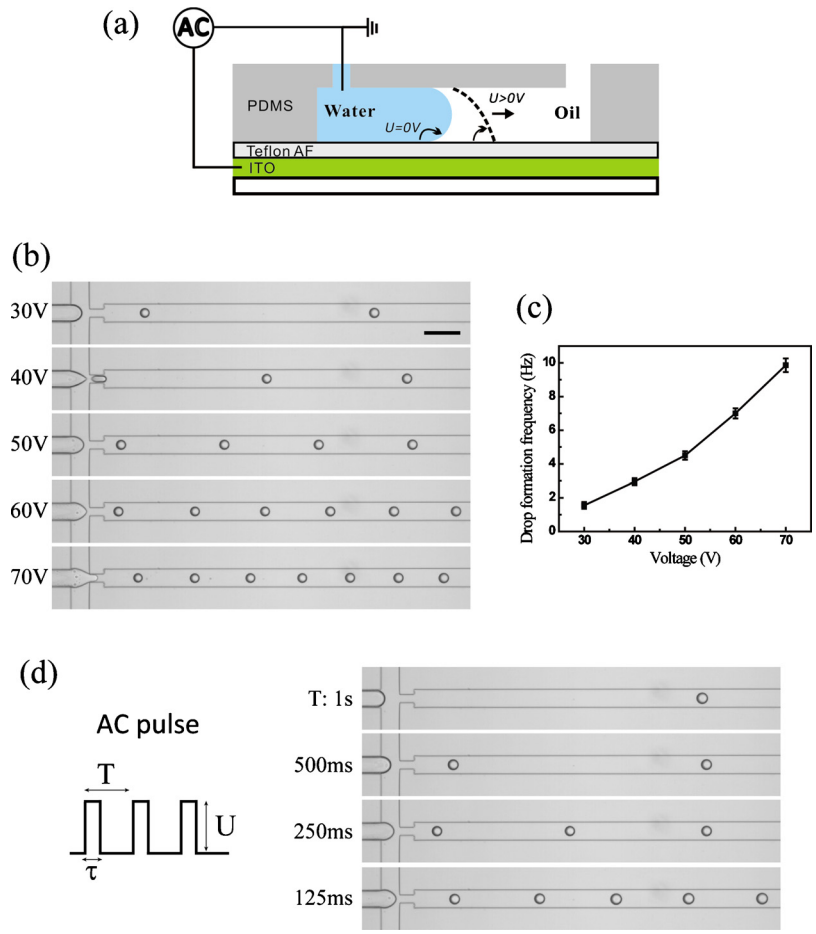

FIG. 1. (a) Schematic side-view illustration of EW-based FFD. When a voltage is applied, the water-oil interface is pulled to the downstream. (b) Drop formation occurs only above a threshold voltage. Increasing U_{rms} further, the drop formation frequency (k) increases while the drop size remains constant. The scale bar is 200 μm. (c) k as a function of U_{rms}. (d) Control over k at fixed U_{rms} by using ac pulses with variable intervals (enhanced online).
[URL: http://dx.doi.org/10.1063/1.3570666.1] [URL: http://dx.doi.org/10.1063/1.3570666.2]
[URL: http://dx.doi.org/10.1063/1.3570666.3] [URL: http://dx.doi.org/10.1063/1.3570666.4]

purely hydrodynamic case, where D and k change simultaneously.[22] It suggests that our electrically induced droplet formation offers separate control over the two quantities. In this scheme, D could be tuned by varying the hydrodynamic conditions via P_W and P_O.

Building on these results, we also explore another DOD mode by fixing U_{rms} at 55 V and using a programmable voltage source to create pulses of width τ and periodicity T. As shown in Fig. 1(d), it is possible to create individual drops (on-demand) by choosing $\tau \approx 120$ ms. The minimum waiting time that allows formation of a similar drop is $T=125$ ms, indicating that any arbitrary pulse sequence with intervals longer than this time will generate a correspondingly timed droplet sequence. Smaller values of τ and T should be obtainable by increasing the hydrostatic pressures.

Mechanistically, the DOD control can be attributed to electrowetting (EW). Applying a voltage U_{rms} over the insulator layer causes the wetting angle θ of the aqueous phase to decrease, according to EW equation $\cos\theta = \cos\theta_Y + \eta$, where θ_Y is the Young's angle and $\eta = CU^2/(2\sigma)$ is the EW number.[23] The increased water wettability of the substrate facilitates the formation (and subsequent break up) of a liquid neck. For the current device with capacitance, $C=3.3$ μF/m^2,

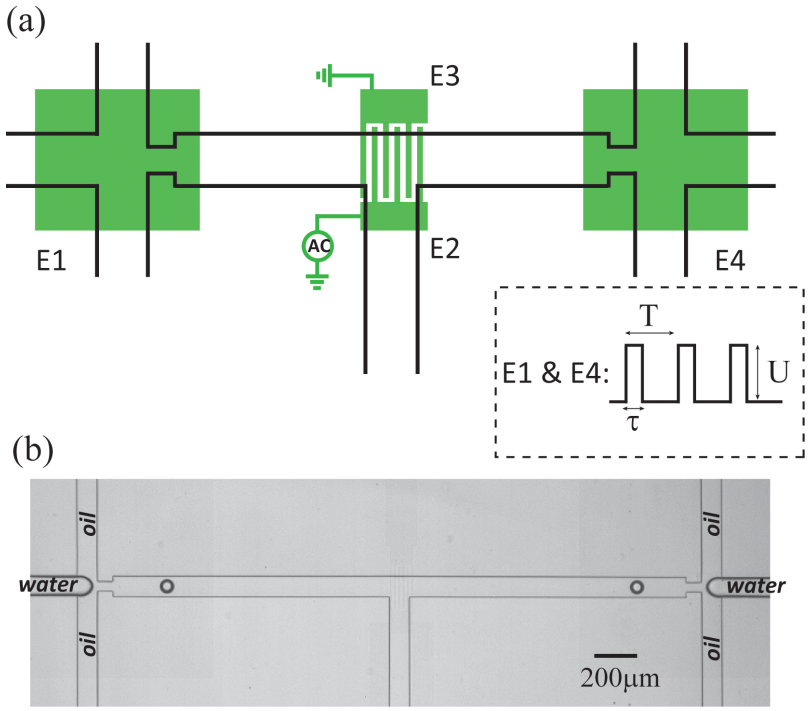

FIG. 2. (a) Schematic of the microfluidic platform for DOD and MOD. Electrodes E1 and E4 are used for triggering drop formation using ac pulses. The IDEs (E2 and E3) are used for merging of droplets. (b) Two droplets are produced simultaneously by switching E1 and E4 at the same time.

and interfacial tension, $\sigma=5$ mN/m, the electric stress and surface tension are equal (i.e., $\eta=1$) for $U\approx 55$ V. Clearly, the EW principle allows to adjust the voltage accordingly for droplets with a different σ.

Merging-on-demand is implemented on the same chip using interdigitated electrodes (IDEs) at a T-junction where the droplets from two DOD injectors meet (see Fig. 2). The IDE stripes have a width of 10 μm and a pitch of 20 μm. To avoid the risk of electrolysis [and possibly also fouling by (bio)molecules inside the drops], we prefer to use isolated electrodes. Since Teflon AF is already used as an insulator for the EW assisted droplet generation, we can simply make use of the same layer to make MOD more reliable. Challenges in the realization of this method are (1) the two drops should arrive simultaneously and (2) the local electric fields at the IDE should be strong enough to destabilize the droplet pair.

Due to the symmetric design, synchronization is simply obtained by applying the same voltage signal to the DOD electrodes E1 and E4. In applications involving asymmetry in the travel time to the junction, compensation could be made by activating E1 and E4 with an appropriate delay time. Merging of droplets is achieved by loading the IDE [E2 and E3 in Fig. 2(a)] with an appropriate (rms) voltage difference ΔU_{rms}. For $\Delta U_{\mathrm{rms}}<20$ V, the electric forces that drive fusion are not strong enough to overcome the resistance of the stabilizing surfactant layers, whereas for $\Delta U_{\mathrm{rms}}\gg 70$ V, electric breakdown of the insulating Teflon layer occurs. One snapshot of two droplets produced simultaneously from opposing flow focusing devices (FFDs) is shown in Fig. 2(b).

If the IDE is switched off, the two droplets do not merge even though they squeeze each other at T-junction [see Figs. 3(a)–3(f)]. This is due to the surfactant stabilization. When merging is chosen, switching on the voltage [i.e., 40 V in the case of Figs. 3(g)–3(l)] destabilizes the surfaces of droplets, resulting in merging (Fig. 3).

To further examine the mechanism of this MOD, we capture images of the critical moments of droplet merging using a high speed camera with a frame rate of 10 000 frames/s. We analyze

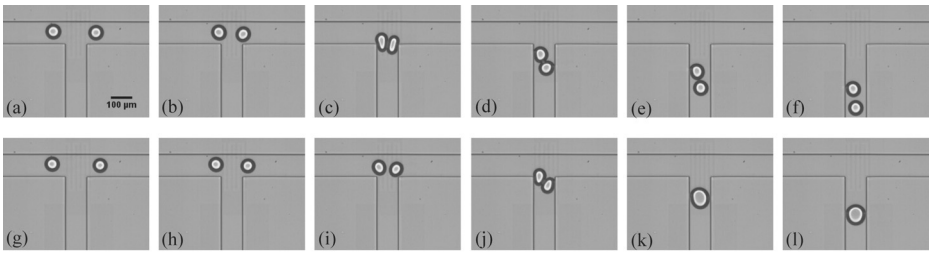

FIG. 3. In sequential images (a)–(f), E2 and E3 are switched off. The droplets meet at the junction and move to downstream without merging; in (g)–(l), E2 and E3 are switched on. Two droplets merge at the junction (enhanced online). [URL: http://dx.doi.org/10.1063/1.3570666.5] [URL: http://dx.doi.org/10.1063/1.3570666.6]

MOD for two devices with the IDE mounted in different orientations relative to the T-junction (see Fig. 4). In Fig. 4(a) (the same orientation of IDE as in Fig. 3), two droplets initially approach each other. The droplets deform and move further downstream in a slightly squeezed configuration imposed by the geometry of the channel walls. Then after an initial increase in separation, suddenly coalescence occurs. The orientation angle at which this happens shows slight variability; this is ascribed to small differences in the arrival time of the two drops at the junction, which affect the subsequent hydrodynamics of the tumbling and approaching droplets. Alternatively in Fig. 4(b), droplets coming from opposite directions touch each other and merge immediately. For both geometries, the qualitative scenarios are highly reproducible and merging occurs with ≈98% efficiency (based on 400 observations). Interestingly, this high efficiency is reached even without a very precisely alignment between IDE and channels.

The merging in our MOD device occurs essentially via electrocoalescence[24] (contributions due to EW and DEP can be rationalized to be weak). In EC, the electric stress $\sigma_E \sim \varepsilon_c \varepsilon_0 E^2$ competes with the capillary pressure $p_c \sim \gamma / R$.[25] σ_E tends to deform (and ultimately disintegrate) the droplet, whereas p_c tends to minimize the interface at constant mean curvature. Significant advances have been made in the understanding of EC.[15,26–28] However, the mechanistic aspects of EC are not yet completely understood even for simple configurations of electrodes and droplets. In our device, the situation is more complex since the electric field due to the IDE is nonuniform at length scales smaller than the droplet diameter. Locally induced droplet deformations are then expected to play a role. This is also suggested by the coalescence events in Fig. 4, which appear to have a preferred alignment with the electrode stripes. In EC, it is common that drop surfaces deform and surfactant layers subsequently become unstable below a certain minimum distance of the surfaces. The role of the external electric field is then to enhance the dynamics of approach and to enlarge the critical distance. This should also apply in our case.

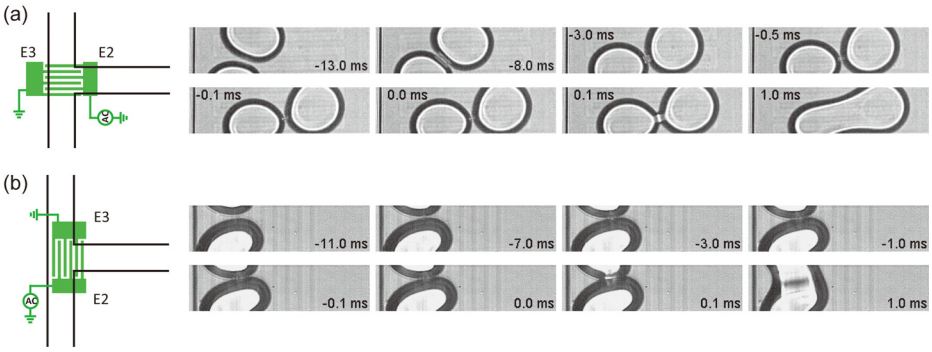

FIG. 4. Sequential images recorded at 10 000 frames/s showing how two droplets merge for different orientations of the IDE stripes. In (a), prior to merging, two droplets contact each other and then rotate until the contact line and electrode stripes have an angle close to 90°. In (b), two droplets merge immediately upon contact. Also, in this case, the contact line has an angle close to 90° with the electrode stripes.

From an application perspective, the physics of electrocoalescence (i.e., the dependence on E, γ, and R) implies that our MOD device can also be made to perform reliably under different conditions (e.g., drop size and interfacial tension) by an up- or downscaling of the geometry or simply by adjusting the voltage.

In conclusion, we demonstrated a microfluidic platform that implements voltage programmable on-demand droplet formation and on-demand droplet merging. DOD is based on electrowetting, while MOD involves electrocoalescence. Our device is easy to fabricate since the number of steps is small and alignment of the IDE is not critical. The device can be operated at relatively low voltages and shows robustness under these conditions. The droplet throughput rate is comparable to other devices. This platform therefore offers interesting perspectives for automated microfluidic screening in various areas of chemistry and biochemistry.

The authors acknowledge support from the MicroNed program, part of the Decree on subsidies for investments in the knowledge infrastructure (Bsik) from the Dutch Government, as well as the research institutes IMPACT and MESA+ at Twente University.

[1] H. A. Stone, A. D. Stroock, and A. Ajdari, Annu. Rev. Fluid Mech. **36**, 381 (2004).
[2] H. Song, D. L. Chen, and R. F. Ismagilov, Angew. Chem., Int. Ed. **45**, 7336 (2006).
[3] Y. C. Tan, K. Hettiarachchi, M. Siu, and Y. P. Pan, J. Am. Chem. Soc. **128**, 5656 (2006).
[4] S. Y. Teh, R. Lin, L. H. Hung, and A. P. Lee, Lab Chip **8**, 198 (2008).
[5] M. Y. He, J. S. Edgar, G. D. M. Jeffries, R. M. Lorenz, J. P. Shelby, and D. T. Chiu, Anal. Chem. **77**, 1539 (2005).
[6] B. C. Lin and Y. C. Su, J. Micromech. Microeng. **18**, 115005 (2008).
[7] S. J. Zeng, B. W. Li, X. O. Su, J. H. Qin, and B. C. Lin, Lab Chip **9**, 1340 (2009).
[8] K. Churski, P. Korczyk, and P. Garstecki, Lab Chip **10**, 816 (2010).
[9] F. Malloggi, S. A. Vanapalli, H. Gu, D. van den Ende, and F. Mugele, J. Phys.: Condens. Matter **19**, 462101 (2007).
[10] F. Malloggi, H. Gu, A. G. Banpurkar, S. A. Vanapalli, and F. Mugele, Eur. Phys. J. E **26**, 91 (2008).
[11] H. Song, J. D. Tice, and R. F. Ismagilov, Angew. Chem., Int. Ed. **42**, 768 (2003).
[12] L. Mazutis, J. C. Baret, and A. D. Griffiths, Lab Chip **9**, 2665 (2009).
[13] X. Niu, S. Gulati, J. B. Edel, and A. J. deMello, Lab Chip **8**, 1837 (2008).
[14] D. R. Link, E. Grasland-Mongrain, A. Duri, F. Sarrazin, Z. D. Cheng, G. Cristobal, M. Marquez, and D. A. Weitz, Angew. Chem., Int. Ed. **45**, 2556 (2006).
[15] C. Priest, S. Herminghaus, and R. Seemann, Appl. Phys. Lett. **89**, 134101 (2006).
[16] W. Wang, C. Yang, and C. M. Li, Small **5**, 1149 (2009).
[17] M. Zagnoni and J. M. Cooper, Lab Chip **9**, 2652 (2009).
[18] M. Zagnoni, G. Le Lain, and J. M. Cooper, Langmuir **26**, 14443 (2010).
[19] M. Zagnoni, C. N. Baroud, and J. M. Cooper, Phys. Rev. E **80**, 046303 (2009).
[20] See http://www.betelco.com/sb/phd/ch5/c52.html for ITO patterning and etching.
[21] E. Seyrat and R. A. Hayes, J. Appl. Phys. **90**, 1383 (2001).
[22] P. Garstecki, H. A. Stone, and G. M. Whitesides, Phys. Rev. Lett. **94**, 164501 (2005).
[23] F. Mugele and J. C. Baret, J. Phys.: Condens. Matter **17**, R705 (2005).
[24] M. Chabert, K. D. Dorfman, and J. L. Viovy, Electrophoresis **26**, 3706 (2005).
[25] A. R. Thiam, N. Bremond, and J. Bibette, Phys. Rev. Lett. **102**, 188304 (2009).
[26] D. H. Michael and M. E. Oneill, J. Fluid Mech. **41**, 571 (1970).
[27] S. Herminghaus, Phys. Rev. Lett. **83**, 2359 (1999).
[28] X. Z. Niu, F. Gielen, A. J. deMello, and J. B. Edel, Anal. Chem. **81**, 7321 (2009).